ELSEVIER

Thermochimica Acta 378 (2001) 27–34

thermochimica acta

www.elsevier.com/locate/tca

Phase behavior of polymer–diluent systems characterized by temperature modulated differential scanning calorimetry

P.C. van der Heijden, M.H.V. Mulder, M. Wessling*

Department of Chemical Technology, Membrane Technology Group, University of Twente, P.O. Box 217, 7500 AE Enschede, The Netherlands

Received 5 February 2001; received in revised form 3 May 2001; accepted 1 June 2001

Abstract

The thermodynamic phase behavior of a polymer–diluent system (atactic polystyrene–1-dodecanol) forms the fundamental basis of the description of thermally-induced demixing processes. In this paper, we demonstrate that temperature modulated differential scanning calorimetry (TMDSC) can accurately detect the liquid–liquid demixing transition. This transition can be clearly observed in the modulus of the complex heat capacity signal and in the phase angle. The phase angle shift is very small during liquid–liquid demixing so liquid–liquid demixing of a polymer–diluent system takes place at time scales instantaneously in comparison with the modulation period of TMDSC. In addition, the glass transition temperature of the polymer-rich phase and the crystallization temperature of the diluent can be determined as well within the same TMDSC experiment.

Keywords: Temperature modulated differential scanning calorimetry; Liquid–liquid demixing; Polymer solution

1. Introduction

Liquid–liquid demixing of binary polymer solutions is extensively studied since the last half of the 20th century (for references, see [1]). Phase diagrams of many polymer–diluent systems have been determined visually or with other optical techniques like optical microscopy (OM) and light scattering [1–7]. These techniques are also used to follow the time dependency of the demixing process to study the kinetics of demixing [7–13]. By using light-based techniques, it is necessary to use a transparent system and the refractive index difference between the polymer and diluent should be large enough to obtain reliable results. Also other experimental techniques have been occasionally used to compose phase diagrams or to follow the demixing process like viscometry [14], NMR [15], X-ray scattering [16] and differential scanning calorimetry (DSC) [17–20]. In this paper, DSC is used for investigating the phase behavior of a polymer solution. By using an alternative technique, measuring heat instead of light, we expect to obtain new insights in the liquid–liquid demixing process. DSC is a well-known experimental technique to study solid–liquid demixing (crystallization) [6,21–23] and vitrification [2,18,19] of liquid–liquid demixed polymer solutions. Berghmans and co-workers [17–20] used DSC as well for the determination of the liquid–liquid demixing temperature. They carried out DSC experiments for the systems atactic polystyrene (aPS)/decalin and atactic polymethylmethacrylate/1-butanol and cyclohexanol,

* Corresponding author. Tel.: +31-53489-2950; fax: +31-53489-4611.
E-mail address: m.wessling@ct.utwente.nl (M. Wessling).

0040-6031/01/$ – see front matter
PII: S0040-6031(01)00587-1

respectively. Upon cooling (cooling rate 5 K min^{-1}), an exothermic heat flow shift was observed and the onset of it was taken as the liquid–liquid demixing temperature. This signal agreed very well with optical observations. With one DSC run they could determine both the liquid–liquid demixing temperature and the glass transition temperature of the polymer-rich phase. But in general, DSC is hardly used for the determination of liquid–liquid demixing because the heat effect is very small and disappears easily in the baseline drift. Recently, a rather new technique has been developed, temperature modulated differential scanning calorimetry (TMDSC) [24,25] which shows a higher sensitivity and is very useful in studying phase transitions in polymeric systems. In spite of some discussion about the interpretation of the measured signals [26–33], TMDSC is a very useful device to measure small heat signals and to separate overlapping thermal events.

In this paper, we will demonstrate that TMDSC allows the accurate determination of the phase diagram of aPS–1-dodecanol, a system showing an upper critical solution temperature behavior. For miscible polymer blends showing lower critical solution temperature behavior, TMDSC has been used in [34]. The TMDSC results are compared with OM. Liquid–liquid demixing temperatures of aPS–cyclohexanol and aPS–diisodecylphthalate are determined as well and compared with literature data. Also the glass transition temperature of the polymer-rich phase and the crystallization temperature of the diluent is measured. For later modeling of the observed heat effects [35], the dependency of the experimental conditions of the TMDSC instrument on the observed signals will be presented. This contribution aims to establish a sound experimental basis for TMDSC in characterizing demixing polymer–diluent systems.

1.1. Temperature modulated DSC

An extensive description can be found in [24,28], a short description of TMDSC will be given below by using these references. With TMDSC, a second function (e.g. a sine wave) is superimposed onto the conventional linear or isothermal temperature ramps. The temperature ramp can then be described as

$$T = T_0 + bt + A\sin\omega t \tag{1}$$

where T_0 (K) is the initial temperature, b (K s^{-1}) the underlying scanning rate, A (K) the temperature amplitude, ω (rad s^{-1}) the angular frequency and t (s) the time.

The resulting heat flow consists of two contributions: the first part is caused by rapid process and is proportional to the scanning rate, while the second part is caused by kinetically hindered or irreversible processes and hence independent of the scanning rate

$$\frac{dQ}{dt} = c_p\frac{dT}{dt} + f(t,T) \tag{2}$$

where dQ/dt (J s^{-1} g^{-1}) is the heat flow, c_p (J g^{-1} K^{-1}) the specific reversing heat capacity and $f(t, T)$ (J s^{-1} g^{-1}) the contribution to kinetic events.

The resulting heat flow can be separated in a cyclic signal and an underlying signal (which is equivalent with the conventional DSC). The modulus of the complex heat capacity ($|c_p^*|$) is calculated with only the amplitude of both the temperature and the heat flow modulation. This modulus of the complex heat capacity can be separated in a part in phase with the modulated temperature and a part out of phase with the help of the phase angle. The kinetic part in Eq. (2) can cause a contribution to the phase angle, but this response can be made insignificantly small by ensuring that there are many cycles within a transition. Consequently, only physical events with a time scale comparable with the modulation period (10–100 s) will be observed in the phase angle [33]. Very fast events, like vibrations and rotations of atoms will take place instantaneously in comparison with a modulation. Slow events, like the mobility of vitrified polymers with time scales much larger than a modulation period will also not influence the phase angle.

2. Experimental

2.1. Materials

Two types of aPS were used: commercial aPS (Styron* 686E) was kindly supplied by Dow Benelux NV (M_w and M_w/M_n : 2.3×10^5 g mol^{-1} and 2.1, respectively, determined with GPC) and aPS synthesized in our own laboratory ($M_w = 6 \times 10^4$ g mol^{-1}, $M_w/M_n = 1.05$) via an anionic polymerization reaction with n-butyl lithium as an initiator [36]. The commercial aPS has been used for the experiments

unless otherwise mentioned. The diluents used, 1-dodecanol (purity >98%, Merck-Schuchardt), diisodecylphthalate (purity >99%, Merck-Schuchardt) and cyclohexanol (purity >99%, Merck-Schuchardt) were used without further purification.

2.2. Sample preparation

A homogeneous solution of aPS and 1-dodecanol was prepared in a three-neck bottle under nitrogen at 200°C. 1-Dodecanol vapor was allowed to evaporate during stirring with a mechanical stirrer. Small amounts of various polymer concentrations were poured in Petri-dishes and cooled in air. The compositions of the samples were determined by thermogravimetric analysis. About 20 mg of the sample was inserted on a platinum sample pan of a TGA 2950 Thermogravic Analyzer of TA Instruments and heated up to 200°C with a heating rate of 10 K min^{-1}. Afterwards, the temperature was kept constant at 200°C for maximum of 2 h to evaporate all the 1-dodecanol. From the ultimate weight loss, the polymer concentration has been determined.

2.3. Temperature modulated differential scanning calorimetry

The TMDSC used is a DSC 2920 of TA Instruments. Calibration with indium and high density polyethylene (HDPE) (for calibration of the heat capacity) has been carried out.

About 5 mg of the sample was put in the aluminum closed sample pan. The TMDSC was heated to 200°C and kept isothermally for 30 min to ensure homogeneity.

The cooling rate was set to 2 K min^{-1} to 0°C and after an isothermal step of 5 min the sample was heated again with 2 K min^{-1}. The amplitude of the superimposed sine wave was 1 K with a period of 60 s (recommended values in the TA Instruments User Manual). The glass transition temperature T_g and the liquid–liquid demixing temperature $T_{L–L}$ as well as the heat capacity shift at $T_{L–L}$ have been determined with the TA Universal Analysis software.

2.4. Optical microscopy

The polymer sample was placed on an object glass within an aluminum ring (thickness 0.1 mm, inner diameter 5 mm) and covered by a second glass. To prevent diluent loss caused by evaporation, laboratory grease was used to stick the aluminum spacer to the object glasses [6]. The sample was placed in a hot stage (Linkam THMS 600) which was controlled by the Linkam TMS92 hot stage controller. The sample has been heated and cooled at a rate of 2 K min^{-1} and demixing was observed visually with an Olympus BH2 microscope (magnification 200×).

3. Results and discussion

3.1. Liquid–liquid demixing and glass transition temperature

In Fig. 1, the result of one TMDSC cooling run is plotted showing the modulus of the complex heat capacity as a function of temperature. The only clearly observed transition in this figure is the crystallization of 1-dodecanol (large peak). The heat effects of vitrification and liquid–liquid demixing can hardly be seen on this scale of modulus of the complex heat capacity.

Cooling and subsequent heating curves of aPS–1-dodecanol without the crystallization peak of the diluent are plotted in Fig. 2 for two polymer concentrations (weight fractions of 0.38 and 0.69). Two transitions can be observed: the glass transition and

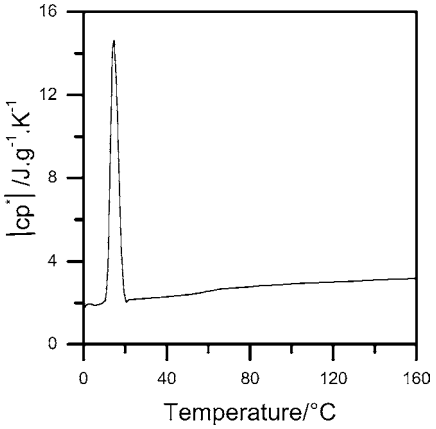

Fig. 1. Modulus of the complex heat capacity as a function of temperature for cooling of aPS in 1-dodecanol (weight fraction of the polymer is 0.38).

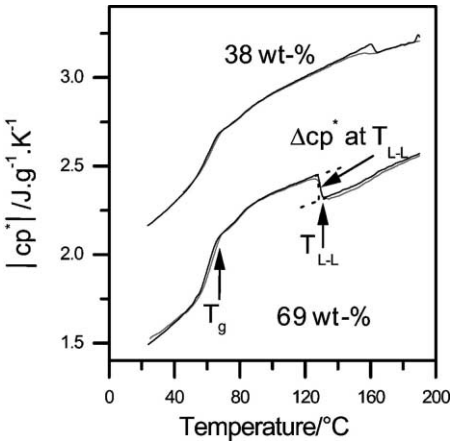

Fig. 2. Cooling and subsequent heating curves (weight fractions of the polymer are 0.38 and 0.69). Grey lines: heating curves, black lines: cooling curves.

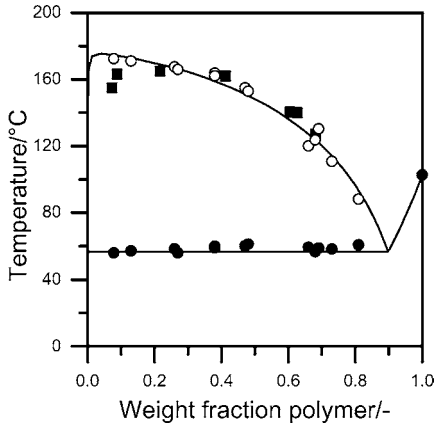

Fig. 3. Phase diagram of aPS–1-dodecanol. Open circles: TMDSC L–L demixing data, closed squares: OM L–L demixing data (cloud points), closed circles: TMDSC glass transition data, lines are drawn to guide the eye.

a small baseline shift at higher temperatures, which we assume to be the liquid–liquid demixing temperature. In the following, we define the onset upon cooling of this signal as the liquid–liquid demixing temperature ($T_{L–L}$) comparable with the observations of Arnauts et al. and Vandeweerdt et al. with the conventional DSC [17–20]. The glass transition temperature (T_g) is chosen as the onset upon cooling because below this temperature we can expect influences of vitrification on the liquid–liquid demixing behavior.

In the cooling curves, the L–L phase transitions at $T_{L–L}$ are represented by a steep heat capacity shift. The heating curves have the same slopes as the cooling curves, only at the liquid–liquid demixing temperatures the transition is not as distinct. A generally observed phenomenon in polymer phase separation is that crystallization peaks are more sharper than melting peaks. With crystallization having a certain degree of supercooling, heat is released instantaneously, while melting shows a more gradual transition with DSC experiments. Liquid–liquid demixing at high polymer concentration is also thought to be influenced by nucleation and growth, hence, supercooling may be present in this transition. However, there is no significant difference observed between the end of the heat capacity shift upon heating and the onset upon cooling, so the physical reason of this observed difference is not completely clear yet. In the following, we will further use and discuss the details of cooling curves only.

Performing such TMDSC cooling experiments over a large concentration range allows the construction of the phase diagram of the polymer–diluent system. To support the assumption of the baseline shift to stem from the L–L demixing, we have compared the TMDSC results with OM data indicating visually the phenomenon of L–L demixing. In Fig. 3, the $T_{L–L}$ and T_g determined with TMDSC and OM is plotted. The open circles represent the TMDSC liquid–liquid demixing data, whereas the filled black squares are the OM data. The closed circles are the glass transition temperature data points.

By assuming the observed demixing temperatures represent the binodal and coexistence curve (only valid for a monodisperse polymer), this phase diagram can be read as follows: by passing the binodal upon cooling, the homogeneous solution will demix in two phases determined by the coexistence curve. With cooling a solution consisting of, e.g. 40 wt.% polymer, a polymer-lean phase consisting of almost pure diluent will be dispersed in a polymer-rich phase determined by the coexistence curve. After further cooling below temperatures of $T = 58°C$, the polymer-rich phase will vitrify (at the intersection between the coexistence curve and the glass transition curve). Cooling of a polymer solution with a weight fraction above 90% will directly result in vitrification of the solution. Further physical explanation of such a phase diagram can be found in many textbooks and papers, such as [37].

At low polymer concentrations (polymer concentrations smaller than 20 wt.%) liquid–liquid demixing observed with OM is located at a somewhat lower temperature than the TMDSC signal. This is probably caused by the small concentration difference of the two co-existing phases at low concentrations, therefore, the refractive index difference of the polymer-rich and polymer-lean phase is very small and difficult to observe visually. The cloud point is thus observed after a certain time later than the actual liquid–liquid demixing resulting in too low temperature measured. At higher concentrations, this problem disappears because the concentration difference between the polymer-rich and polymer-lean phase is larger and L–L demixing is more easy to observe visually.

The experimental error of both techniques will also have an influence, in particular the evaporation of diluent. TMDSC experiments with a mass loss larger than 0.2 mg after experimentation were omitted. With the OM experiments, the average error in the temperature was 4°C, averaged over six experiments. But in spite of the small deviation between the TMDSC and OM data, we can conclude that the observed heat capacity shift is indeed caused by liquid–liquid demixing. The observed $T_{L–L}$'s with TMDSC can be regarded as the cloud point curve of the polymer solution at a high polymer concentration (larger than about 20 wt.%).

3.2. Liquid–liquid demixing for aPS–cyclohexanol and aPS–diisodecylphthalate

TMDSC results of aPS in cyclohexanol and diisodecylphthalate, respectively, are plotted in Fig. 4. The concentration of polystyrene is 30 wt.%. These cloud points observed with TMDSC compare well with reported values of these systems. Song and Torkelson [38] observed liquid–liquid demixing for a 20 wt.% aPS ($M_w = 2.9 \times 10^5\,g\,mol^{-1}$) in cyclohexanol solution at $T_{L–L} = 80.5$°C (our work with the TMDSC: $T_{L–L} = 81.4$°C). Nojima et al. [8] determined the cloud point of aPS ($M_w = 1.1 \times 10^5\,g\,mol^{-1}$, $M_w/M_n < 1.06$) with diisodecylphthalate at $T_{L–L} = 47$°C for 30 vol.% (TMDSC: $T_{L–L} = 49.7$). The glass transition of aPS–diisodecylphthalate is not observed from the DSC curve because this transition is at a lower temperature than the temperature interval of the experiment. From this comparison between experimental and reported data it can also be concluded that

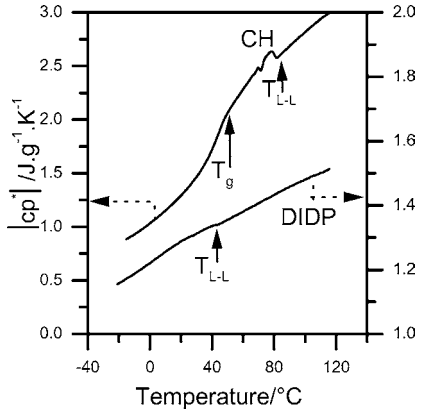

Fig. 4. Modulus of the complex heat capacity of aPS in diisodecylphthalate (DIDP) and cyclohexanol (CH). Weight fraction of polymer is 0.30 for both curves.

the measured heat capacity shift has to be caused by liquid–liquid demixing. The difference in values in the heat capacity shift (Δc_p^* at $T_{L–L}$, defined in Fig. 2) between the different diluents is caused by the interaction between polymer and diluent. This can be quantified by calculating the enthalpy of mixing with the help of the Flory–Huggins theory [20]. More details about the quantification of this heat capacity shift will be published later [35].

3.3. TMDSC results of aPS (M_w/M_n is 1.05) with 1-dodecanol

Fig. 5 shows the experimental result of a cooling run for aPS having a low M_w/M_n (M_w is $6 \times 10^4\,g\,mol^{-1}$, M_w/M_n is 1.05) in 1-dodecanol (mass fraction of aPS is 0.40). The $T_{L–L}$ shows a lower value than the value plotted in Fig. 3 for a poly-disperse aPS–1-dodecanol system (151 and 157°C, respectively). This experimental finding is in accordance with theory [1], since the molecular weight of the sample with a low M_w/M_n (M_w is $6 \times 10^4\,g\,mol^{-1}$) is smaller than the poly-disperse sample (M_w is $2.3 \times 10^5\,g\,mol^{-1}$).

3.4. Influence of experimental conditions on modulus of the complex heat capacity

To minimize the error in the calculation of the modulus of the complex heat capacity with the TMDSC software, it is recommended that at least four complete superimposed cycles fit within a phase

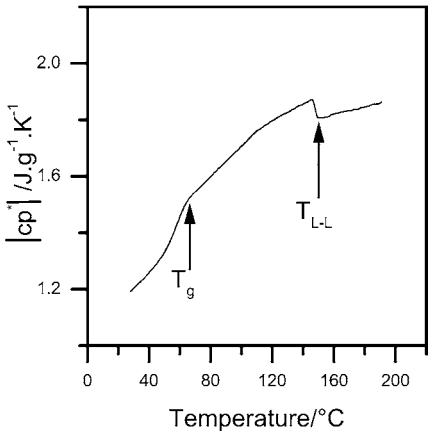

Fig. 5. Modulus of the complex heat capacity versus temperature of aPS ($M_w = 6 \times 10^4$ g mol^{-1}, M_w/M_n is 1.05) in 1-dodecanol. Weight fraction of polymer is 0.40.

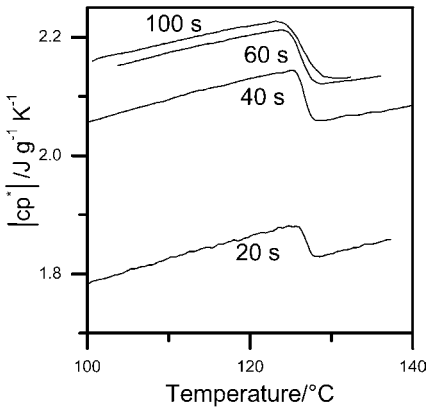

Fig. 7. Influence of modulation period on modulus of complex heat capacity. Weight fraction of polymer is 0.68.

transition (according to Manual TA Instruments). This requirement is satisfied for the glass transition because this transition covers a temperature range of at least 10 K. However, in case of liquid–liquid demixing the heat capacity shift only covers a temperature interval of 2 K, so only one modulated cycle fits within this transition. By lowering the underlying cooling rate, the number of cycles within the transition can be increased; the resulting DSC curves are shown in Fig. 6. From this figure it can be concluded that cooling rates of 2 K min^{-1} and lower has no significant influence on the measured modulus of the complex heat capacity.

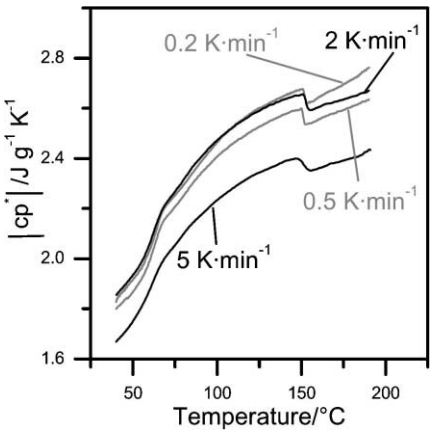

Fig. 6. Influence of cooling rate on modulus of the complex heat capacity. Weight fraction of polymer is 0.48.

The results given in this paper are all measured with a modulation period of 60 s. Of course, it would be of much interest to study the influence of the modulation period on the modulus of the complex heat capacity. Such information may reveal details on the time scale of liquid–liquid demixing. The results of the TMDSC experiments with different modulation periods are plotted in Fig. 7.

As can be observed from Fig. 7, the experiments with the lower modulation periods (20 and 40 s) have much lower modulus of the complex heat capacity values compared to the higher modulation periods (60 and 100 s), even in the homogeneous solution region. The values of the heat capacity for the experiments with a modulation period of 60 and 100 s give comparable results; so from these results we may conclude that at lower modulation periods the system cannot follow the modulation. The observed difference is not caused by physical phenomena in the sample because in the homogeneous solution it is not expected that thermal events of these periods take place; this has to be caused by the time lag of the TMDSC instrument (caused by heat transfer in the furnace and the sample). Therefore, high modulation periods (>60 s) are necessary to exclude the instrumental time lag.

Plotting the phase angle versus the temperature (Fig. 8), one can observe that the phase angle shifts to lower values for increasing modulation period. As already mentioned, there is a time lag in the TMDSC instrument, and in general, the phase shift caused by

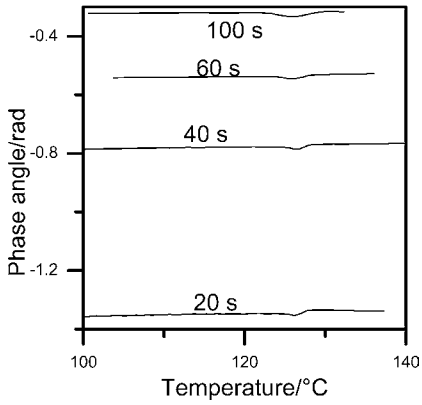

Fig. 8. Influence modulation period on phase angle. Weight fraction of polymer is 0.68.

the instrument is very large in comparison with the phase shift caused by physical events of the polymer–diluent system.

A method to exclude the influence of the phase angle shift caused by the TMDSC instrument from the total phase angle is to define regions in the DSC curve where no influence of physical events is expected, so where the phase angle has to be zero. By assuming that the polymer–diluent sample shows no contribution on the phase angle in the region where the polymer is vitrified [28], we can exclude the contribution of the phase shift caused by the TMDSC instrument. For all polymer concentrations, the phase angle change caused by the polymer–diluent system are only about 0.08 rad over the temperature interval from 30 to 200°C and it shows besides a peak at T_g, a small peak at $T_{L–L}$ of about 0.005 rad. So, the influence of the out of phase contribution is very small at $T_{L–L}$ and the modulus of the complex heat capacity can indeed be regarded as the reversing heat capacity. The shift in the heat capacity has to be caused by phenomena of a time scale instantaneously in comparison with the modulation period; liquid–liquid demixing takes place at time scales instantaneously in comparison with the modulation period of TMDSC.

4. Conclusions

With TMDSC liquid–liquid demixing of polymer–diluent systems can be determined as well the glass transition of the polymer-rich phase and crystallization of diluent in one run. Both the modulus of the complex heat capacity and the phase angle show a signal at the demixing temperature. Liquid–liquid demixing observed with TMDSC agrees well with visually observed cloud points. The underlying cooling rate must be 2 K min^{-1} or lower and the modulation period must be above 60 s to be sure that the experimental set-up has no influence on the results. The phase angle shift is very small during liquid–liquid demixing so liquid–liquid demixing of a polymer–diluent system takes place at time scales instantaneously in comparison with the modulation period of TMDSC.

Acknowledgements

We thank Ruurd Lammers, Johan Bos and Elwin Schomaker of Akzo Nobel Central Research in Arnhem for their support to use the TMDSC apparatus and extensive discussions and Daniel Brooke (Akzo Nobel) for carrying out part of the experiments. Mark Hempenius (University of Twente) is acknowledged for synthesizing the near monodisperse polystyrene sample and Clemens Padberg (University of Twente) for the GPC experiments to determine the molecular weight distribution.

References

[1] R. Koningsveld, A.J. Staverman, J. Polym. Sci. A 6 (1968) 349.
[2] R.M. Hikmet, S. Callister, A. Keller, Polymer 29 (1988) 1378.
[3] F.J. Tsai, J.M. Torkelson, Macromolecules 23 (1989) 775.
[4] C.L. Jackson, M.T. Shaw, Polymer 31 (1990) 1070.
[5] D.R. Lloyd, S.S. Kim, K.E. Kinzer, J. Membr. Sci. 64 (1991) 1.
[6] S.S. Kim, D.R. Lloyd, Polymer 33 (1992) 1047.
[7] B.J. Cha, K. Char, J.-J. Kim, S.S. Kim, C.K. Kim, J. Membr. Sci. 108 (1995) 219.
[8] S. Nojima, K. Shiroshita, T. Nose, Polym. J. 14 (1982) 289.
[9] J. Lal, R. Bansil, Macromolecules 24 (1991) 290.
[10] A. Laxminarayan, K.S. McGuire, S.S. Kim, D.R. Lloyd, Polymer 35 (1994) 3060.
[11] K.S. McGuire, A. Laxminarayan, D.R. Lloyd, Polymer 36 (1995) 4951.
[12] P.D. Graham, A.J. Pervan, A.J. McHugh, Macromolecules 30 (1997) 1651.
[13] J. Szydlowski, W.A. Van Hook, Macromolecules 31 (1998) 3255.
[14] B.A. Wolf, M.C. Sezen, Macromolecules 10 (1977) 1010.
[15] G.T. Caneba, D.S. Soong, Macromolecules 18 (1985) 2538.

[16] Y. Xie, K.F.J. Ludwig Jr., R. Bansil, P.D. Gallagher, Č. Koňák, G. Morales, Macromolecules 29 (1996) 6150.
[17] J. Arnauts, H. Berghmans, Polym. Commun. 28 (1987) 66.
[18] P. Vandeweerdt, H. Berghmans, Y. Tervoort, Macromolecules 24 (1991) 3547.
[19] J. Arnauts, H. Berghmans, R. Koningsveld, Makromol. Chem. 194 (1993) 77.
[20] J. Arnauts, R. De Cooman, P. Vandeweerdt, R. Koningsveld, H. Berghmans, Thermochim. Acta 238 (1994) 1.
[21] J.H. Aubert, Macromolecules 21 (1988) 3468.
[22] K.E. Kinzer, D.R. Lloyd, Polym. Mater. Sci. Eng. 61 (1989) 794.
[23] L. Aerts, M. Kunz, H. Berghmans, R. Koningsveld, Macromol. Chem. 194 (1993) 2697.
[24] M. Reading, Trends Polym. Sci. 1 (1993) 248.
[25] M. Reading, B.K. Hahn, B.S. Crowe, Patent 5 224 775, TA Instruments, Inc. (1993).
[26] T. Ozawa, K. Kanari, Thermochim. Acta 253 (1995) 183.
[27] J.E.K. Schawe, Thermochim. Acta 260 (1995) 1.
[28] K.J. Jones, I. Kinshott, M. Reading, A.A. Lacey, C. Nikolopoulos, H.M. Pollock, Thermochim. Acta 304/305 (1997) 187.
[29] G.W.H. Höhne, Thermochim. Acta 304/305 (1997) 121.
[30] J.E.K. Schawe, Thermochim. Acta 304/305 (1997) 111.
[31] B. Wunderlich, A. Boller, I. Okazaki, K. Ishikiriyama, Thermochim. Acta 304/305 (1997) 125.
[32] R. Scherrenberg, V. Mathot, P. Steeman, J. Thermal Anal. 54 (1998) 477.
[33] R. Scherrenberg, V. Mathot, A. Van Hemelrijck, Thermochim. Acta 330 (1999) 3.
[34] G. Dreezen, G. Groeninckx, S. Swier, B. Van Mele, Polymer 42 (2001) 1449.
[35] P.C. van der Heijden, M.H.V. Mulder, M. Wessling, submitted to Macromolecules.
[36] D.J. Worsfold, S. Bywater, Can. J. Chem. 38 (1960) 1891.
[37] V.B.F. Mathot, Calorimetry and Thermal Analysis of Polymers, Hanser, Munich, 1994, p. 227.
[38] S.-W. Song, J.M. Torkelson, J. Membr. Sci. 98 (1995) 209.